Journal of Organometallic Chemistry, 277 (1984) 335–350
Elsevier Sequoia S.A., Lausanne – Printed in The Netherlands

SYNTHESIS, CRYSTAL AND MOLECULAR STRUCTURE, AND DYNAMIC STEREOCHEMISTRY OF $CH_2[(C_6H_5)Sn(SCH_2CH_2)_2NCH_3]_2$, A COMPOUND WITH TWO FIVE-COORDINATE TIN CENTERS

RUDOLPH WILLEM, MARCEL GIELEN,

AOSC-TW, Vrije Universiteit Brussel, Pleinlaan 2, B-1050 Brussel (Belgium)

JACQUELINE MEUNIER-PIRET, MAURICE VAN MEERSSCHE,

Laboratoire de Chimie-Physique et de Cristallographie, Université de Louvain, Bâtiment Lavoisier, Place Louis Pasteur, 1, B-1348 Louvain-la-Neuve (Belgium)

KLAUS JURKSCHAT and ALFRED TZSCHACH

Department of Chemistry, Martin-Luther University, Weinberg 16, 4020 Halle a.d. Saale (German Democratic Republic)

(Received July 6th, 1984)

Summary

The crystal and molecular structure of $CH_2[(C_6H_5)Sn(SCH_2CH_2)_2NCH_3]_2$ were determined by X-ray diffraction. Both tin atoms show approximate trigonal-bipyramidal coordination, but the two phenyl rings and the methylene bridge do not occupy the same sites around the two metal centers.

The ^1H, ^{13}C, ^{119}Sn data at various temperatures and magnetic fields indicate the presence in the slow exchange region of three isomers. The observations are interpreted on the basis of the assumption that in solution the phenyl groups can occupy both equatorial positions, both axial positions or one axial and one equatorial position. The last combination which is observed in the solid state, corresponds to the major isomer in solution. The stereochemical correspondence between this system and six-coordinate *cis*-bis-chelate complexes of the type $M(AB)_2X_2$ is outlined. In the fast exchange region the spectra show that only one residual isomer is present. These observations imply that in the main isomerization process the tin atoms rearrange independently of each other. The data indicate that this rearrangement proceeds through the dissociation-inversion mechanism previously discussed.

Introduction

Pentacoordinated organotin compounds have been intensively investigated in the last 15 years. Besides synthetic aspects, the question of the validity of the polarity

0022-328X/84/$03.00

rule and mechanistic concepts to account for interconversion pathways have been the subject of considerable interest [1]. Compounds containing two pentacoordinated tin centers within one molecule are still rare [2–4], but they provide interesting models for discussion of the stereochemistry of pentavalent structures. The recent development of methods for making functionalized bis(organostannyl)methanes having unusual complexing properties [5–8] offers the possibility of preparing such compounds with tridentate ligands. We present below the results of studies on the solid state structure and the dynamic stereochemistry in solution of CH_2-$[(C_6H_5)Sn(SCH_2CH_2)_2NCH_3]_2$, which was prepared from $[CH_2(PhSnO)_2]_n$ and $CH_3N(CH_2CH_2SH)_2$ in refluxing toluene.

Crystal and molecular structure

The structure of the compound $CH_2[(C_6H_5)Sn(SCH_2CH_2)_2NCH_3]_2$ (**1**) is shown in Fig. 1. Each tin atom exhibits distorted trigonal bipyramidal geometry. The bridging methylene group is in an apical position in the Sn(1) environment but is equatorial in the Sn(2)-coordination sphere. The phenyl groups likewise occupy either an equatorial or an apical site, whereas the nitrogen atoms are both apical. Fractional coordinates and selected interatomic distances and angles are given in Tables 1 and 2. As expected for trigonal bipyramidal environments, the two Sn–C bonds located in apical positions (i.e. Sn(1)–C(1) and Sn(2)–C(8)) are longer than the corresponding bonds in equatorial positions (Sn(2)–C(1) and Sn(1)–C(2)), but this effect is stronger for the phenyl groups. The Sn–C and Sn–S bond lengths can be compared with those of similar compounds [9–12]. Both tin–nitrogen bond lengths are close to but longer than the Sn–N distances in 2,2,6-trimethyl-1,3-dithia-6-aza-2-stannaocane [9,10], in methylthiostannatrane [11] and in pentacarbonyl[5-t-butyl-5-aza-2,8-dithia-1-stannabicyclo[3.3.$0^{1,5}$]octane]chromium [12] (2.65 Å instead of 2.40 in the chromium complex). It is noteworthy that changing the distribution of the organic groups around the trigonal bipyramid evidently does not affect the Lewis-acidity of the tin atoms. Table 3 lists the torsion angles describing the conformation of the two eight-membered rings and also some angles between mean planes. One ring (that involving Sn(1)) adopts a boat-chair conformation, and the

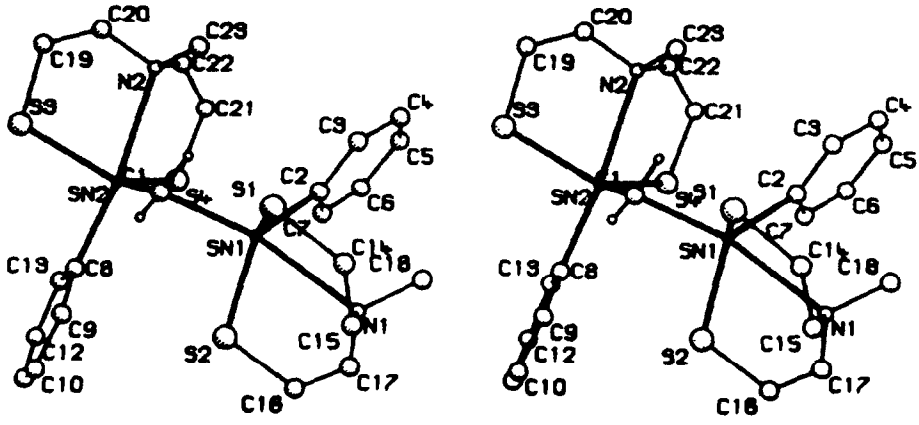

Fig. 1. A stereoview of the molecule with atom-numbering scheme.

TABLE 1

FRACTIONAL ATOMIC COORDINATES ($\times 10^4$) WITH e.s.d's IN PARENTHESES

	x	*y*	*z*
Sn(1)	1353(1)	1057(0)	1889(0)
Sn(2)	1054(1)	911(0)	3617(0)
S(1)	−891(3)	1568(2)	1051(1)
S(2)	3896(3)	1774(2)	2338(1)
S(3)	−731(4)	1184(2)	4354(1)
S(4)	2841(3)	−288(2)	3828(1)
N(1)	2753(11)	1190(6)	888(4)
N(2)	−1112(10)	−321(5)	3385(4)
C(1)	95(11)	1340(6)	2651(4)
C(2)	1769(10)	−240(5)	1833(4)
C(3)	628(11)	−751(6)	1435(4)
C(4)	1012(12)	−1615(6)	1388(4)
C(5)	2451(13)	−1933(7)	1755(5)
C(6)	3569(13)	−1419(7)	2172(5)
C(7)	3227(12)	−566(6)	2191(4)
C(8)	2960(11)	1803(6)	4037(4)
C(9)	3032(12)	2600(6)	3761(5)
C(10)	4237(15)	3161(8)	4033(5)
C(11)	5431(15)	2931(8)	4571(6)
C(12)	5408(15)	2179(8)	4853(6)
C(13)	4136(13)	1605(7)	4593(5)
C(14)	3(14)	1739(9)	348(5)
C(15)	1796(15)	1858(8)	495(5)
C(16)	4997(17)	1798(13)	1688(7)
C(17)	4434(17)	1403(19)	1150(6)
C(18)	2666(20)	403(11)	509(8)
C(19)	−2278(18)	349(9)	4219(8)
C(20)	−2257(28)	−211(14)	3787(12)
C(21)	1500(19)	−1156(7)	3664(11)
C(22)	−166(21)	−1055(9)	3610(17)
C(23)	−2027(20)	−415(10)	2713(7)
H(1)	154(113)	1843(66)	2638(40)
H(2)	−901(115)	1071(56)	2280(45)

other ring is apparently midway between the boat–chair and chair–chair conformation. Such an intermediate conformation was previously described for $C_6H_5(Cl)Sn(SCH_2CH_2)_2O$ [13] and $(C_6H_5)_2Sn(SCH_2CH_2)_2O$ [14].

The two shortest intermolecular contacts are (a) S(1)...C(21) 3.78 Å; (b) S(2)...C(6) 3.61 Å. These are too long for C–H...S hydrogen bonds.

NMR Results

The ^1H spectra of compound **1** in $CDCl_3$ recorded at room temperature on 270 and 500 MHz spectrometers display numerous overlapping signals in the region 0–3 ppm, with variable intensities and exhibiting badly resolved couplings to tin. The aromatic region displays a similarly complex pattern. The spectra indicate that compound **1** exists as a mixture of isomers on this time scale. The ^1H spectrum recorded at room temperature on a 60 MHz spectrometer shows broad coalescing

TABLE 2

SELECTED INTERATOMIC DISTANCES (Å) AND BOND ANGLES (°)

S(1)–Sn(1)	2.423(2)	S(3)–Sn(2)	2.424(2)
S(2)–Sn(1)	2.409(2)	S(4)–Sn(2)	2.418(2)
N(1)–Sn(1)	2.654(7)	N(2)–Sn(2)	2.651(7)
C(1)–Sn(1)	2.162(7)	C(1)–Sn(2)	2.153(7)
C(2)–Sn(1)	2.129(8)	C(8)–Sn(2)	2.179(8)
C(14)–S(1)	1.833(10)	C(19)–S(3)	1.838(12)
C(15)–C(14)	1.460(15)	C(20)–C(19)	1 294(18)
C(15)–N(1)	1.482(13)	C(20)–N(2)	1.423(15)
C(16)–S(2)	1.819(11)	C(21)–S(4)	1.775(12)
C(17)–C(16)	1.307(20)	C(22)–C(21)	1.368(20)
C(17)–N(1)	1.423(16)	C(22)–N(2)	1.443(16)
C(18)–N(1)	1.499(17)	C(23)–N(2)	1.475(15)
Sn(2)–S(2)	4.213(2)	Sn(1)–S(4)	4.592(2)
C(1)–Sn(1)–N(1)	162.8(3)	C(8)–Sn(2)–N(2)	166.4(3)
S(2)–Sn(1)–S(1)	126 2(1)	S(4)–Sn(2)–S(3)	117.4(1)
C(2)–Sn(1)–S(1)	113.6(2)	C(1)–Sn(2)–S(3)	114.4(2)
C(2)–Sn(1)–S(2)	110.9(2)	C(1)–Sn(2)–S(4)	121.1(2)
C(1)–Sn(1)–S(1)	93.7(2)	C(8)–Sn(2)–S(3)	95.9(2)
C(1)–Sn(1)–S(2)	97.1(2)	C(8)–Sn(2)–S(4)	95.4(2)
C(2)–Sn(1)–C(1)	111.1(3)	C(8)–Sn(2)–C(1)	105.2(3)
N(1)–Sn(1)–S(1)	77.2(2)	N(2)–Sn(2)–S(3)	76.9(2)
N(1)–Sn(1)–S(2)	77.4(2)	N(2)–Sn(2)–S(4)	78.2(2)
C(2)–Sn(1)–N(1)	86.0(3)	C(1)–Sn(2)–N(2)	88.4(3)

signals, indicating that at this field isomer conversion becomes rapid on the NMR time scale. At 97°C the spectrum, at 80 MHz, of **1** in C_6D_5Br exhibits two patterns in the aromatic region, one between 6.82 and 7.45 ppm, obscured by residual signals of C_6D_5Br and a well defined one between 7.64 and 7.76 ppm arising from the *ortho*-phenyl protons coupled to tin ($^3J \simeq 60$ Hz). In the region 0 to 3 ppm, the

TABLE 3

TORSION ANGLES (°) IN THE EIGHT-MEMBERED RINGS AND ANGLES BETWEEN MEAN-PLANES

Angle		Angle	
S(2)–Sn(1)–S(1)–C(14)	60	S(3)–Sn(2)–S(4)–C(21)	70
Sn(1)–S(1)–C(14)–C(15)	−23	Sn(2)–S(4)–C(21)–C(22)	−15
S(1)–C(14)–C(15)–N(1)	54	S(4)–C(21)–C(22)–N(2)	30
C(14)–C(15)–N(1)–C(17)	−166	C(21)–C(22)–N(2)–C(20)	−139
C(15)–N(1)–C(17)–C(16)	86	C(22)–N(2)–C(20)–C(19)	109
N(1)–C(17)–C(16)–S(2)	25	N(2)–C(20)–C(19)–S(3)	3
C(17)–C(16)–S(2)–Sn(1)	−6	C(20)–C(19)–S(3)–Sn(2)	−1
C(16)–S(2)–Sn(1)–S(1)	−69	C(19)–S(3)–Sn(2)–S(4)	−69
N(1)–Sn(1)–S(1)–C(14)	−3	N(2)–Sn(2)–S(4)–C(21)	1
N(1)–Sn(1)–S(2)–C(16)	−5	N(2)–Sn(2)–S(3)–C(19)	0
S(1)–Sn(1)–N(1)–C(15)	28	S(4)–Sn(2)–N(2)–C(22)	10
S(1)–Sn(1)–N(1)–C(17)	147	S(4)–Sn(2)–N(2)–C(20)	123
S(2)–Sn(1)–N(1)–C(15)	−105	S(3)–Sn(2)–N(2)–C(22)	−112
S(2)–Sn(1)–N(1)–C(17)	15	S(3)–Sn(2)–N(2)–C(20)	1

spectrum displays the expected signals for a unique averaged isomer: one CH_3-N signal at 1.58 ppm, without coupling to tin, a complex pattern likewise uncoupled for the CH_2-N protons between 2.20 and 2.34 ppm, another complex pattern for the CH_2-S protons, between 2.52 and 2.80 ppm and showing a satellite pattern arising from tin coupling ($^3J \simeq 45$ Hz), and a singlet at 0.96 ppm, with the expected coupling, arising from the CH_2 bridge between the tin atoms ($^2J(^{119}Sn-^1H)$ 66 Hz; $^2J(^{117}Sn-^1H)$ 64 Hz).

Chemical shift data from selected ^{13}C spectra recorded on various spectrometers, at several temperatures, are given in Table 4. Spectra at high temperatures and low fields are indicative of a unique averaged residual isomer.

These spectra exhibit well defined expected couplings: $^2J(C_{ortho}-Sn)$ 48 Hz; $^3J(C_{meta}-Sn)$ 68 Hz; $^3J(CH_2N-Sn)$ 54 Hz; $^2J(CH_2S-Sn)$ 31 Hz. The coupling between the CH_3-N and tin is not observed, while the CH_2-Sn and C_{ipso} signals are too weak and too broad to give observable satellites. In the slow exchange region two signals having different intensities are observed for the CH_2-S, CH_3-N, $Sn-CH_2-Sn$ resonances. Two weak resonances attributable to the C_{ipso} are also observed above 143 ppm; they are all quite broad, however, and so coupling could not be observed at 125 MHz. Below room temperature, at $-20°C$, only the CH_2N signal splits further, but we could not unambiguously observe the slow exchange couplings. In the coalescence region the $Sn-CH_2-Sn$ and C_{ipso} resonances disappear in the noise. The splitting of each unique ^{13}C signal of the fast exchange region into two signals in the slow exchange region is attributed to an isomerization process between isomers becoming slow on the observational time scale. The ^{119}Sn NMR data confirm this. Spectra recorded at 32°C in $CDCl_3$ at 74.63 MHz display 4 signals in ratio 0.8/1/1/0.2 at -4.10, -15.59, -21.50 and -31.68 ppm, respectively, relative to Me_4Sn as external reference. The signals at -15.59 and -21.50 ppm exhibit a $^2J(^{119}Sn-C-^{119}Sn)$ coupling of 193 Hz whereas the other two are too broad to show a coupling. At 120°C, in *p*-xylene-d_{10}, a unique, broad residual resonance at -10.46 ppm is observed.

TABLE 4

^{13}C CHEMICAL SHIFTS, IN ppm TOWARDS TMS OF COMPOUND **1**. WHERE NECESSARY INTENSITIES ARE GIVEN IN PARENTHESES.

Field (MHz)	Temperature (°C)	Solvent	$Sn-CH_2-Sn$	CH_2S	CH_3-N	CH_2-N	C_{ipso}	C_{ortho}	C_{meta} C_{para}
22.63	25	$CDCl_3$	–	24.4	42.4 (2) 43.2 (1) broad	58.7	–	134.8	128.3 broad
20.12	60	$CDCl_3$	–	24.3	42.7 broad	58.7	–	134.7	127.9 broad
20.12	125	C_6D_5Br [a]	11.7 weak	24.2	42.3	58.7	146.4 weak	134.7	–
125.72	25	$CDCl_3$	10.5 (2) 15.6 (1) weak	24.1 (1) 24.5 (2)	42.4 (2) 43.6 (1)	58.7 broad	143.1 149.6 weak	134.6	127.4 –128.8 several signals

[a] The chemical shifts for **1**, in C_6D_5Br were calculated from the chemical shift of C_{ortho} assuming $\delta_{C_{ortho}} = 134.7$ ppm. In this spectrum $C_{meta/para}$ signals overlap with those of C_6D_5Br.

TABLE 5

^{119}Sn AND ^{13}C NMR DATA OF COMPOUNDS **2** AND **3** (The spectra were recorded at 304 K in $CDCl_3$ on a 200 MHz spectrometer: 74.63 MHz for ^{119}Sn and 50.29 MHz for ^{13}C. The ^1J coupling of the *ipso* carbon of isomer (b) of compound **2** could not be observed. The ^{13}C signals of isomer (b) of compound **2** were less intense than those of isomer (a) by at least a factor 3)

Compound		^{119}Sn	
		Chemical shifts δ(ppm),$(CH_3)_4Sn$	Intensity ratio
$(C_6H_5)(CH_3)Sn(SCH_2CH_2)_2NCH_3$ (**2**)	Isomer (a)	−10.76	1
	Isomer (b)	−32.40	2
$(C_6H_5)_2Sn(SCH_2CH_2)_2NCH_3$ (**3**)		−69.9	–

		^{13}C			
		CH_3–Sn		C_{ipso}	
		δ(ppm), TMS	^1J(Sn–C) (Hz)	δ(ppm), TMS	^1J(Sn–C) (Hz)
$(C_6H_5)(CH_3)Sn(SCH_2CH_2)_2NCH_3$ (**2**)	Isomer (a)	0.24	499	149.85	434
	Isomer (b)	4.31	356	143.91	–
$(C_6H_5)_2Sn(SCH_2CH_2)_2NCH_3$ (**3**)		–	–	149.36	489
				141.38	700

For comparison with compound **1**, we also prepared $(C_6H_5)CH_3Sn(SCH_2CH_2)_2NCH_3$ (compound **2**) and $(C_6H_5)_2Sn(SCH_2CH_2)_2NCH_3$ (compound **3**) [15]. Their NMR data are given in Table 5. The data for compound **2** indicate that this derivative exists as a mixture of two isomers, a minor one, (b) and a major one (a). Those for compound **3** indicate that only one isomer is present, containing two diastereotopic phenyl groups.

Stereochemistry

Scope

Consider a hypothetical five-coordinate trigonal bipyramidal compound surrounded by five different monodentate achiral ligands, labelled 1 to 5. It can easily be shown [16–18] that in this situation of general ligand partition [19,20] ten diastereomeric pairs of enantiomers are possible. The easiest way to symbolize these 20 isomers is to specify them by using the two labels of the axial ligands, in natural order. Looking from the axial ligand with smallest label, the labels of the three equatorial ligands appear in arithmetic order, either clockwise or counterclockwise. In the latter case the symbol of the isomer is $\overline{ij}$, in the former ij, with $i < j$, in which i and j are the labels of the two axial ligands [16–20]. The symbols of the twenty possible isomers are therefore 12,$\overline{12}$, 13,$\overline{13}$, 14,$\overline{14}$, 15,$\overline{15}$, 23,$\overline{23}$, 24,$\overline{24}$, 25,$\overline{25}$, 34,$\overline{34}$, 35,$\overline{35}$, 45,$\overline{45}$. When some of the ligands are identical in chemical nature, i.e. in a situation of particular ligand partition [19,21], the number of possible isomers is, of course, reduced. An easy way of finding them is to attribute identical labels to identical ligands and to see which ones of the 20 isomer symbols of the general

ligand partition collapse. Furthermore, in some five-coordinate compounds [17,18], chemical constraints such as orientation rules related to electronegativity or the presence of cyclic ligands make some of the 20 isomers of the general ligand partition impossible. An example is *N*-methyl-5,5-dialkyldiptychthiaazastannolidine [22] (Fig. 2). In this molecule the chemical constraints are induced both by the higher electronegativity of nitrogen with respect to carbon and sulfur and by the cyclic structure of the tridentate ligand. Because of this the nitrogen occupies an axial position and both sulfur atoms equatorial ones [22–26]. This means that if R = 1, R′ = 2, N = 3 and both sulfurs are labelled 4 and 5, only four configurations from the 20 above remain possible: 13,$\overline{13}$, 23 and $\overline{23}$ resulting in two achiral isomers when R ≠ R′, 13 and 23, since the sulfur atoms 4 and 5 are constitutionally identical (4 = 5).

In the case R = R′, the species 13 and 23 further collapse to the unique isomer symbol 13, since now 1 = 2. For R = R′ = Me and R = R′ = t-Bu the configurations

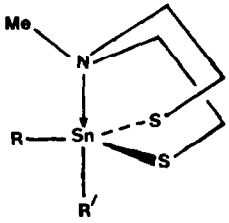

Fig. 2. The structure of *N*-methyl-5,5-dialkyldiptychthiaazastannolidines.

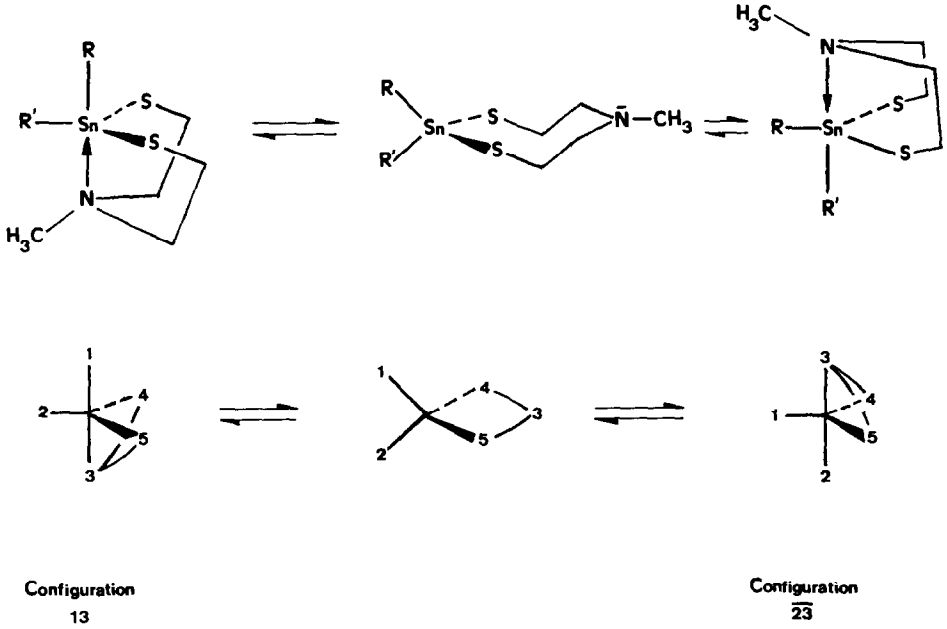

Fig. 3. The dissociation–inversion mechanism. The schematic representation at the bottom of the figure indicates which conversion of configurations of a trigonal bipyramid is implied by this mechanism.

13 and $\overline{23}$ (or $\overline{13}$ and 23) were shown to be converted into one another. The proposed mechanism, a dissociation–inversion mechanism [22–26], is shown in Fig. 3 for $R \neq R'$ but is equally valid for $R = R'$

For R = Me and R′ = t-Bu additional steric requirement makes one of the isomers 13 or 23 energetically unfavourable, so that no isomerization could be observed. Because of the very low apicophilicity of the t-butyl group, studied intensively in the case of five-coordinate phosphorus compounds [27], the isomer having the t-butyl groups in equatorial position is preferred, although the values of coupling constants between protons and tin do not allow conclusions to be drawn concerning which isomer is actually retained in solution [22].

Static stereochemistry of ***1*** *in solution*

The aspect of compound **1** in which we are interested concerns the special situation in which: (1.) R and R′, although different, can occupy both apical and equatorial positions; (2.) there are two five-coordinate centers. Both must now be characterized by a symbolism of the type described above, so that a double symbolism indicates now which ligands occupy axial positions at both tin centers. To do so, we number the ligands on the tin atom as follows: the methylene bridge: 1, both phenyl groups: 2 and 2′; N-Me: 3 and 3′; and the sulfurs: 4,5, and 4′5′. Taking into account the chemical constraints mentioned above, three isomers are possible. They are represented schematically in Fig. 4, together with two types of symbols. The first symbolism is a natural extension of the usual symbolism specified above for one-center five-coordination. It is the most useful symbolism for discussing the

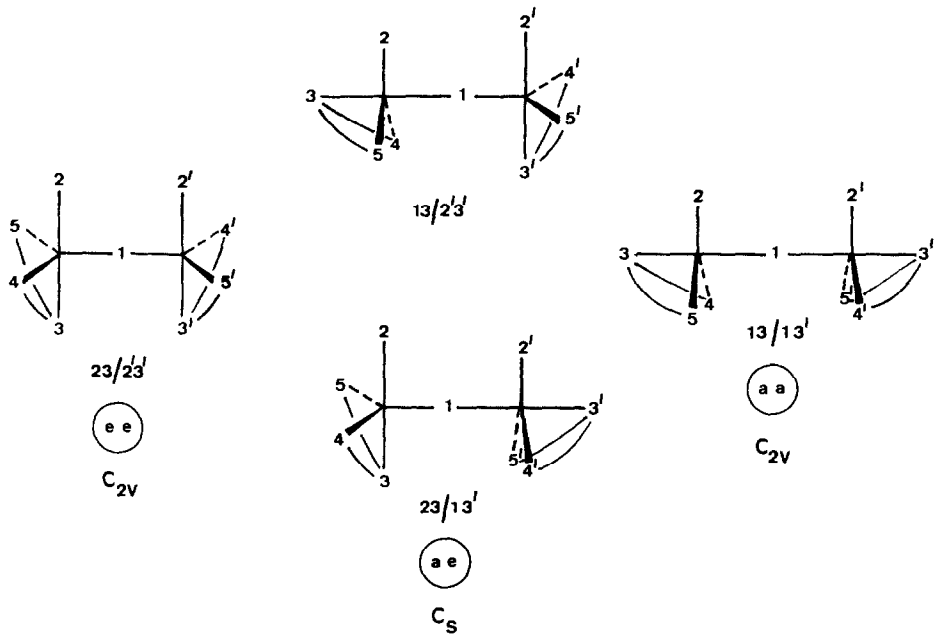

Fig. 4. The three possible isomers of **1**, their symbols and symmetry. The isomer *ae* can be represented by two different pairs of configurations, $\overset{(-)}{13}/\overset{(-)}{2'3'}$ and $\overset{(-)}{23}/\overset{(-)}{13}$, while the isomers *ee* and *aa* each correspond to a single pair of configurations.

five-coordination features of the static and dynamic stereochemistry of this compound (**1**). It should be noted that when 4 and 5 are permuted the configuration symbols represented should bear a bar. The other, less explicit symbols refer to the position of the methylene bridge on both tin atoms to which it is bound: *a* = *axial*; *e* = *equatorial*. The isomer *ae* can be represented by two different configuration symbols, 13/23′ and 23/13′ because its symmetry number is only 1 instead of 2 for the isomers *ee* and *aa*. Its statistical weight is therefore twice that of the others. It is interesting to note that there is a stereochemical correspondence [28–30] between the isomers above and those of a six-coordinate bis-chelate system of the type *cis*-$M(AB)_2X_2$ [31,32] for instance $Sn(bzac)_2Cl_2$, bzac = benzoylacetonate (see Fig. 5). In this context the second symbolism is the most useful.

Figures 4 and 5 establish this correspondence. The correspondence of **1** to *cis*-$M(AB)_2X_2$ relies on the following comparison. The metal M of $M(AB)_2X_2$ is in correspondence to the carbon of the methylene bridge between the tin atoms of compound **1**; the two X groups of $M(AB)_2X_2$ correspond to the two hydrogens of the methylene bridge of **1**. Finally both dissymmetric chelates AB are in correspondence with both five-coordinate tin centers. More precisely, if we call A the chelate moiety bearing the substituent A and bound to the metal M of $M(AB)_2X_2$, then the two possible angles A–M–X can be either both 180° (both A *trans* to or *equatorial* with X; isomers ΔAA and ΛAA) or one 180° (*trans* or *equatorial*) and one 90° (*cis* or *axial*; isomers ΔAB and ΛAB) or both 90° (both A *cis* to or axial with X; isomers ΔBB and ΛBB). In compound **1** the angles C–Sn–N can be both 180° (isomer *aa*), one 180° and one 90° (isomer *ae*) or both 90° (isomer *ee*). In other words, the correspondence between the isomers of $M(AB)_2X_2$ and compound **1** are established by the value (180° or 90°) of both angles A–M–X and N–Sn–CH_2 respectively: 180°–180°: ΔAA and ΛAA ↔ *aa*; 180°–90° or 90°–180°: ΔAB and ΛAB ↔ *ae*, with double statistical weight; 90°–90°: ΔBB and ΛBB ↔ *ee*. It should be stressed that this correspondence is one between pairs of enantiomers for $M(AB)_2X_2$ and achiral isomers for compound **1**. This difference arises from the fact that the skeletons of six-coordinate bis-chelates are chiral while those of compound **1** are all achiral.

Indeed for each of the isomers *aa*, *ae*, *ee* of compound **1** it is possible to find one rotamer in which the local symmetry plane of the tridentate ligand, which also contains the Sn–Ph bond, coïncides with the plane formed by the bonds Sn–CH_2–Sn. Therefore if free rotation about all the C–Sn bonds is assumed, as is reasonable, the three isomers have, at least on the NMR time scale, one symmetry plane. When, in addition, the configurations about both tin atoms are now identical, then an additional C_2 axis and σ_v plane result (isomers *aa* and *ee*).

Dynamic stereochemistry

cis-Bis-chelates $M(AB)_2X_2$ can rearrange according to three types of modes of rearrangements [31–33], $\overset{(-)}{M}_0$, $\overset{(-)}{M}_1$ and $\overset{(-)}{M}_2$. M_j occurs without and $\overline{M}_j$ with inversion of Λ or Δ configuration ($j = 0$, 1 or 2) while $\overset{(-)}{M}_j$ symbolizes indifferently M_j, $\overline{M}_j$ or both. The modes $\overset{(-)}{M}_0$, $\overset{(-)}{M}_1$ and $\overset{(-)}{M}_2$ exchange the A and B moieties within respectively no, one and two chelate bridges of $M(AB)_2X_2$ simultaneously. M_0 is the trivial

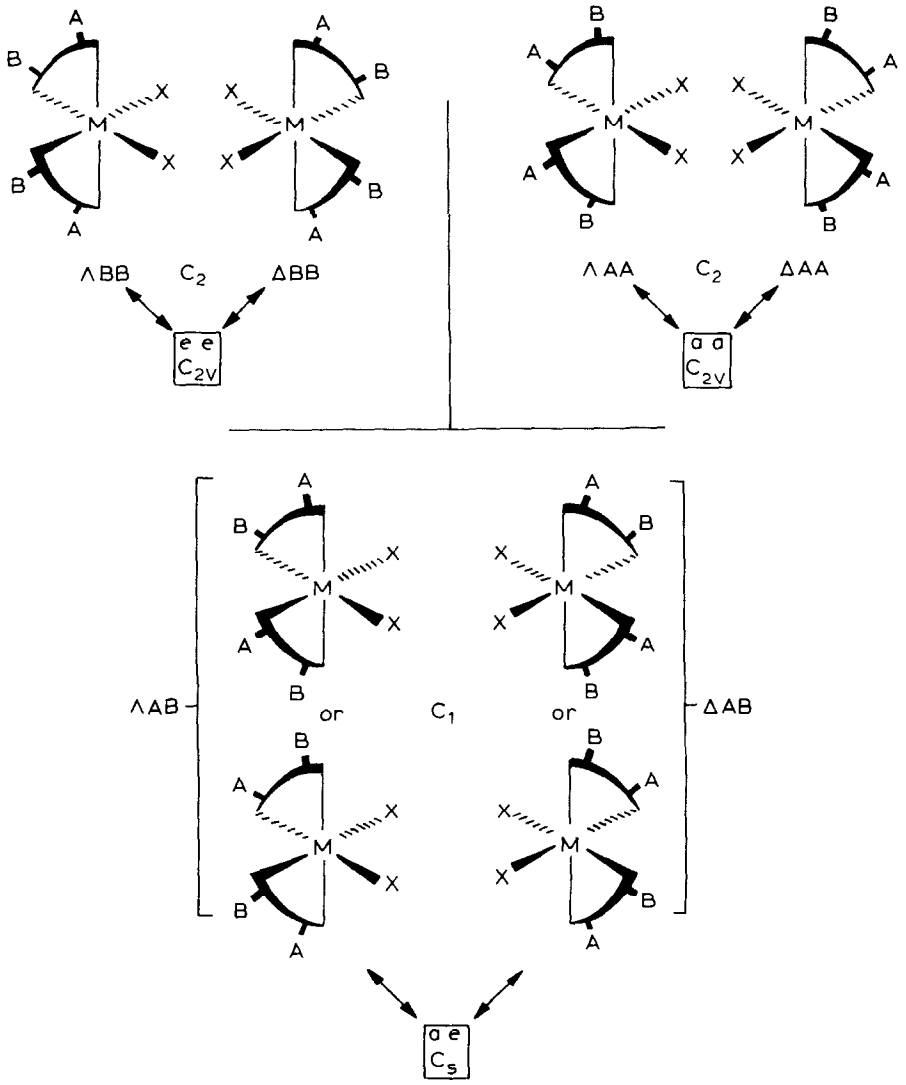

Fig. 5. The three diastereomeric pairs of enantiomers of a six-coordinate bis-chelate complex of the type $M(AB)_2X_2$ and their stereochemical correspondence to the achiral isomers of compound **1**.

identity while $\overline{M}_0$ results in an enantiomerization without diastereomerization. The mode $\overset{(-)}{M}_2$ can be performed in only one way, since there is only one pair of chelates that can undergo a permutation of their moieties simultaneously. In contrast, since there are two ways of permuting the chelate moieties of only one chelate bridge, the mode $\overset{(-)}{M}_1$ can be performed through two pathways. When applied to the isomers AA and BB these two pathways of $\overset{(-)}{M}_1$ are symmetry equivalent because of the C_2 axis, but when applied to the isomer AB they are symmetry unequivalent because the C_2

axis is lost, and accordingly these two pathways generate two different isomers [31–33]. The stereochemical correspondence [28–30] established for the static stereochemistry of $M(AB)_2X_2$ and **1** is equally valid for their dynamic stereochemistry. As a natural extension of this idea we define the three modes of rearrangements M_0, M_1 and M_2 for compound **1**. The distinction between M_j and $\overline{M}_j$ is irrelevant in this case since the molecules are achiral on the NMR time scale, and M_0, M_1 and M_2 mean that isomerization can proceed at zero, one, and two five-coordinate tin centers respectively. The ways in which these modes convert the possible isomers of compound **1** into each other can be described by matrices. We associate a matrix Π^α with the mode M_α. The row and column indices i and j of the matrix Π^α represent isomers. The matrix element Π^α_{ij} for the mode M_α is defined as

$\Pi^\alpha_{ij} = n$ when isomer i is converted into isomer j by n pathways of mode M_α

$\Pi^\alpha_{ij} = 0$ when no conversion from i to j proceeds by mode M_α.

The matrices Π^0, Π^1, Π^2 associated with the modes M_0, M_1, M_2 are respectively:

$$\Pi^0 = \begin{array}{c|ccc} & aa & ee & ae \\ aa & 1 & 0 & 0 \\ ee & 0 & 1 & 0 \\ ae & 0 & 0 & 1 \end{array}; \quad \Pi^1 = \begin{array}{c|ccc} & aa & ee & ae \\ aa & 0 & 0 & 2 \\ ee & 0 & 0 & 2 \\ ae & 1 & 1 & 0 \end{array}; \quad \Pi^2 = \begin{array}{c|ccc} & ae & ee & ae \\ aa & 0 & 1 & 0 \\ ee & 1 & 0 & 0 \\ ae & 0 & 0 & 1 \end{array}$$

Π^0 is the trivial identity matrix representing no isomerization and is not discussed further. The matrix representing M_1, Π^1, describes the uncorrelated isomerization of only one tin-center at a time while Π^2 represents the correlated isomerization of both tin centers simultaneously. The block diagonal structure of Π^2 indicates that not all three isomers are converted into each other by mode M_2: the two C_{2v} isomers are converted into one another, the C_s isomer is converted into itself. The use of matrices in which the isomer labels are replaced by the configuration labels of Fig. 4 gives a better insight into the way by which these isomerizations relate the different possible five-coordinate centers. This is particularly the case for isomer *ae*, since it is composed of two pairs of possible configurations which are exchanged by mode M_2.

$$\Pi'^2 = \begin{array}{c|cc} & \overset{(-)\ (-)}{13/2'3'} & \overset{(-)\ (-)}{23/13'} \\ \overset{(-)\ (-)}{13/2'3'} & 0 & 1 \\ \overset{(-)\ (-)}{23/13'} & 1 & 0 \end{array}$$

Thus the isomerization of *ae* into itself by mode M_2 corresponds to an exchange of the two distinguishable five-coordinate tin centers. In contrast the non-block diagonal character of the matrix Π^1 shows that the mode M_1 mixes up the three possible isomers completely into a unique residual isomer. In this uncorrelated isomerization each of the tin centers can isomerize independently. Therefore, for any isomer, the mode M_1 can be performed in two ways, as shown by the fact that the sum of the matrix elements of Π^1, on a given row, is two.

Our ^{119}Sn NMR data indicate the presence of these three isomers in the slow exchange region ($T < 303$ K). The two central intense signals, the relative intensities of which remain equal over the whole temperature range examined, are attributed to the isomer *ae* in which the tin atoms are diastereotopic. The two lateral signals, the intensities of which vary differently with temperature with respect to the central

signals, are attributed to the isomers *aa* and *ee* in which both tin atoms are homotopic. We attribute the smaller of these two signals to the isomer *ee*, which is easily seen from molecular models to be the most sterically crowded, but we have no direct evidence for this. The coalescence of these four signals to a unique averaged one at 373 K is incompatible with the mode M_2 alone. When M_2 is rapid on the ^{119}Sn NMR time-scale, a coalescence to two averaged signals must result: one results from the exchange of the isomers *aa* and *ee*, and the second one from the exchange of the two diastereotopic tin centers within the isomer *ae* (configuration exchange $\overset{(-)}{2}\overset{(-)}{3}/\overset{(-)}{1}\overset{(-)}{3}' \rightleftharpoons \overset{(-)}{1}\overset{(-)}{3}/\overset{(-)}{2}\overset{(-)}{3}'$).

In contrast, the complete mixing of the isomers by mode M_1 must result in a unique averaged signal, as is observed. Therefore our observed unique averaged signal can be attributed to the mode M_1 but also to a combination of modes M_1 and M_2, the mode M_2 alone being excluded. If mode M_1 alone proceeds, each tin center isomerizes independently from the other one. If the mixture of modes $M_1 + M_2$ is responsible for the coalescence, then of course both correlated and uncorrelated isomerizations do proceed but the correlated isomerization cannot be more rapid than the uncorrelated one.

The ^{1}H and ^{13}C NMR data above the coalescence limit can also be explained unambiguously in terms of a unique residual isomer. The slow exchange ^{1}H spectra display too many overlappings between 0 and 3 ppm to be interpreted easily. The ^{13}C data in the slow exchange region are interpreted as follows: (1) The presence of only two Sn–CH_2–Sn signals instead of the three expected for a mixture of three isomers is attributed to the low intensity of these signals together with the low molar fraction of the third isomer and/or to partial signal averaging or broadening. (2) For the CH_2N, CH_3N, CH_2S and C_{ipso} resonances, four signals are in principle expected, one for each C_{2v} isomer, 2 for the C_s isomers. The fact that only two are observed for CH_2N, CH_2S and C_{ipso} is readily explained either by partial averaging or, more likely, by the fact that the chemical shift of these carbons is sensitive only to the configurational environment of the tin atom to which they are bound, but not to that of the other tin atom. In this way, only one axial C_{ipso} signal arises from the isomer *ee* and *ae* together and only one equatorial signal from the isomer *aa* und *ae*; analogously, the chemical shift of the CH_3-N group would depend only on the phenyl group or the CH_2 bridge occupies the other axial site, similar arguments holding for the CH_2S and CH_2N resonances. Note that in the latter case, the chemical shift difference is so small that only a broad signal is observed at room temperature.

The NMR results for compound **2** can be interpreted in terms of a mixture of trigonal bipyramidal isomers, such as those shown in Fig. 2 and 3. Because of the larger coupling constant of the methyl group to tin in the major isomer (a) (^1J(Sn–C) 499 Hz) than in the minor isomer (b) (^1J(Sn–C) 356 Hz) we assign isomer (a) to the one having the methyl group in the equatorial and the phenyl group in the axial position (R = Ph, R′ = Me; Ph = 1, Me = 2, configuration 13 in Fig. 3) and, accordingly the isomer (b) to the one with the equatorial phenyl group and the axial methyl group (configuration $\overline{23}$ in Fig. 3). These results reflect the expected slightly larger apicophilicity in solution of a phenyl group compared with a methyl group, the apicophilicity order being therefore t-Bu < Me < Ph.

Mechanistic considerations

We suggest that the mechanism by which these isomers are interconverted is the dissociation–inversion process proposed previously [22–26] and presented in Fig. 3. The absence of $^3J(H_3C-N-Sn)$ couplings in the ^1H and ^2J coupling in the ^{13}C fast exchange NMR spectra indicate that rupture of the bond between Sn and N has become rapid on the NMR time scale. This is confirmed by the absence of the CH_2-N coupling in the fast exchange ^1H spectrum. The maintenance at high temperature of the $^{13}C-^{119}Sn$ coupling of the CH_2-N group is readily explained by a ^3J coupling through the equatorial sulfur atoms. Therefore the mechanism of Fig. 3 provides likely explanation of our results. Figure 3 is applicable to compound **1** provided ligand 1 represents the CH_2 group along with its other tin moiety, which is assumed to remain rigid during the isomerization on the considered tin atom, since the isomerization has been shown to be essentially uncorrelated. We discuss this isomerization further in terms of the idealized modes of rearrangements of five coordinate trigonal bipyramidal skeletons presented elsewhere [18–20]. It has been shown [18–20] that the isomerization of Fig. 3, from configuration $\overline{13}$ to configuration 23 (or from 13 to $\overline{23}$) corresponds to the idealized mode of rearrangements $\hat{P}_2$ of the trigonal bipyramid. It is clearly seen here that $\hat{P}_2$ can be decomposed into a single axial–equatorial exchange (mode $\hat{P}_3$) [35] combined to an inversion at the metal center (mode $\hat{P}_5$) [35] i.e. that $\hat{P}_2 = \hat{P}_3 . \hat{P}_5$ as shown previously [20]. It is worth mentioning that this rearrangement does not have the same stereochemical character as the Berry mechanism [36], which belongs to the idealized mode $\hat{P}_1$ [17–20,35]. The Berry mechanism is incompatible with the loss of couplings observed in the fast exchange ^1H and ^{13}C spectra. Moreover, it cannot relate directly the only possible isomers of compound **1**, since the configurations 13 and $\overline{23}$ (or $\overline{13}$ and 23) are not directly related by the mode $\hat{P}_1$ [17–20,35]. Therefore Berry pseudorotations would be only possible, as shown previously [18], through a sequence of two rearrangements of mode $\hat{P}_1$: $13 \rightleftharpoons 45 \rightleftharpoons \overline{23}$ involving an intermediate 45 in which both sulfur atoms are axial, and, consequently, the nitrogen equatorial; this is a highly energetic structure which is incompatible with polarity rules, as shown previously [22–26].

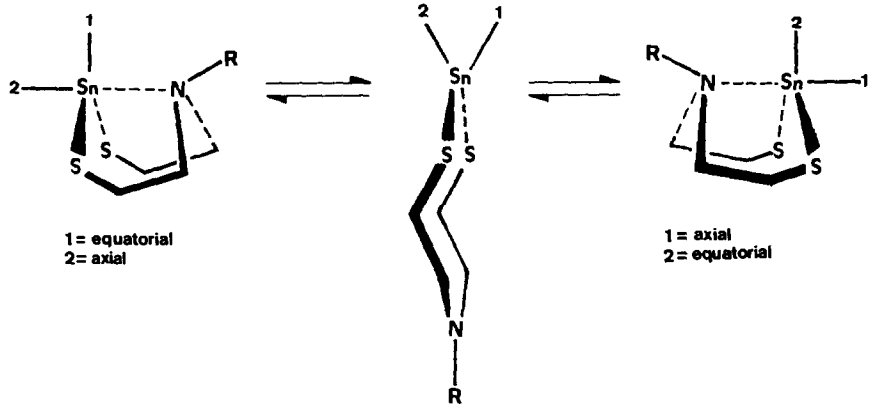

Fig. 6. Boat conformation inversion with axial–equatorial exchange of the dissociation–inversion mechanism in compound **1**.

This is, however, not the only reason why compound **1** rearranges through the mode $\hat{P}_2$ rather than mode $\hat{P}_1$, which is the most usual for five-coordination [34]. We relate this also to the very special nature of the process we are concerned with, which is clearly less related to configurational rearrangements at five-coordinate metal centers than to inversion mechanisms of heterocycles; the dissociation–inversion mechanism must essentially be seen as the inversion of a kind of boat conformation of a 1-stanna-2,7-dithia-5-azacyclooctane derivative in which the tin and nitrogen atoms interact. Figure 6 shows that this results in an axial-equatorial exchange at tin with inversion at the latter.

Therefore the stereochemistry of compound **1** is more relevant to conformational ring rearrangements than to rearrangements at five-coordinate metal centers.

Mössbauer results

The ^{119}Sn Mössbauer spectrum of **1** shows an isomer shift of 1.19 mm/s and a quadrupole splitting of 1.15 mm/s. Like in the HMPA complexes of $(Ph_2XSn)_2CH_2$ [37] the expected difference of 0.18 mm/s in the QS values of both tin atoms (i.e. 1.12 mm/s for Sn(1) and 1.30 mm/s for Sn(2); calculation according to the method described in ref. 23) is not observed.

Anti-cancer activity

The in vivo anti-tumour activity [40] of **1** (NSC 370456) against P388 lymphocytic leukaemia in CDF_1 mice was evaluated in accordance with standard protocols for primary screening [41]. Ratios T/C of medium survival times (days) of treated and untreated mice are equal to 100% for doses from 50 mg/kg to 200 mg/kg. It can therefore be concluded that **1** is inactive and not toxic.

Experimental

Synthesis of 1

To a suspension of 3.6 g (8.2 mmol) $[CH_2(PhSnO)_2]_n$, prepared by alkaline hydrolysis of $(PhBr_2Sn)_2CH_2$ [8], in 300 ml of toluene $MeN(CH_2CH_2SH)_2$ (2.5 g, 16.4 mmol) was added. The mixture was refluxed with vigorous stirring. After 2 h the solvent was evaporated and the residue recrystallized from benzene to give a white, crystalline solid, m.p. 85–87°C, yield 5 g (86%). Analysis. Found: C, 39.55; H, 4.82; N, 4.03. $C_{23}H_{34}N_2S_4Sn_2$ calcd.: C, 39.24; H, 4.83; N, 3.98%.

The mass spectrum of **1** contains in addition to a very small molecular ion the fragment ions (*m/e*, intensity, possible structural formula) as shown in Table 6.

Crystal structure

$Sn_2S_4N_2C_{23}H_{34}$ crystallizes in space group $P2_1/c$ with a 8.279(2), b 16.146(6), c 21.331(9) Å, β 102.72°, V 2781 Å^3, M_{rel} 704.2, μ 19.5 cm^{-1}, D_c 1.681 g cm^{-3} ($Z = 4$).

Reflections were recorded with a Syntex $P2_1$ diffractometer using graphite-monochromatized Mo-K_α (λ 0.71069 Å), 2θ maximum was 47°; of the 4127 reflections 3457 (with $I > 2.5\sigma(I)$) were considered as observed, no absorption corrections were applied. The Sn(1) position was found from a Patterson map and other non-H atoms from DIRDIF [38]. The refinement was carried out with SHELX program [39] to a

TABLE 6

MASS SPECTRUM of compound 1

m/e	Intensity	Possible structural formula
629	14	$CH_2Sn_2C_6H_5(SCH_2CH_2N(CH_3)CH_2CH_2S)_2$
569	1	$CH_2Sn_2C_6H_5(S)(SCH_2CH_2N(CH_3)CH_2CH_2S)$
557	0.5	$CH_2Sn_2(C_6H_5)_2(SCH_2CH_2N(CH_3)CH_2CH_2S)$
515	1	$CH_2Sn_2(C_6H_5)(SCH_2)_4$
494	1	$Sn(C_6H_5)_2(SCH_2CH_2N(CH_3)CH_2)(SCH_2CH_2N(CH_3)CH_2CH_2)$
483	1	$Sn(C_6H_5)_2(SCH_2CH_2N(CH_3)CH_2CH_2S)SCH_2CH_2$
481	1	$CH_2Sn_2(SCH_2CH_2N(CH_3)CH_2CH_2S)(SCH_2)S$
422	2	$Sn(C_6H_5)_2SCH_2CH_2N(CH_3)CH_2CHS$
385	3	$SnH(SCH_2CH_2N(CH_3)CH{=}CH_2)(SCH_2CH_2N(CH_3)CH_2CHS)$
372	3	$Sn(SCH_2CH_2N(CH_3)CH_2CH_2S)(SCH_2CH_2N(CH_3)CH_2)$
360	6	$Sn(C_6H_5)(SCH_2CH_2N(CH_3)CH_2CH_2S)CH_2$
346	100	$C_6H_5Sn(SCH_2CH_2N(CH_3)CH_2CH_2S)$
300	11	$C_6H_5SnSCH_2CH_2N(CH_3)CH_2$
269	18	$Sn(SCH_2CH_2N(CH_3)CH_2CH_2S)$
229	9	C_6H_5SnS
223	4	$SnSCH_2CH_2N(CH_3)CH_2$
209	7	$SnSCH_2CH_2NCH_3$
208	7	$SnSCH_2CH_2NCH_2$
197	27	C_6H_5Sn
120	13	Sn

final conventional *R* value of 0.048 (for 3457 observed reflections). The final atomic positional parameters are listed in Table 1, in which the numbering of Fig. 1 is used. Tables of observed and calculated structure factors and a list of temperature factors may be obtained from one of the authors (JMP).

NMR Spectra

The ^1H NMR spectra at room temperature were recorded on Varian T60 and Bruker AM500 and HX270 spectrometers. The high temperature ^1H spectra were recorded on a Bruker WP80 spectrometer. The ^{13}C spectra at room temperature were recorded at 22.63 and 125.72 MHz on Bruker WH90 and AM500 spectrometers respectively. The high temperature ^{13}C spectra were recorded on a Jeol SX100 apparatus. The ^{119}Sn spectra were recorded at 74.63 MHz with a Bruker WP200 spectrometer.

Acknowledgements

We thank Dr. D. Zimmerman for recording ^1H NMR spectra at high temperature, Dr. R. Dommisse and Dr. A. Jans for recording ^{13}C NMR spectra, Dr. C. Mügge for recording ^{119}Sn NMR spectra, Mr. M. De Smet for recording mass spectra, and Dr. B. Mahieu for recording the Mössbauer spectra. Useful discussions with Ir. H. Pepermans are gratefully acknowledged. Two of us (R.W. and M.G.) are grateful to Dr. Yoder and Dr. Atassi (Bordet Institute, Brussels) for the screening experiments performed under the auspices of the Developmental Therapeutics Program, Division of Cancer Treatment, National Cancer Institute Bethesda, Maryland.

References

1 A. Tzschach and K. Jurkschat, Comments Inorg. Chem., 3 (1983) 35.
2 K. Kawakami, M. Miya-Uchi and T. Tanaka, J. Organomet. Chem., 70 (1974) 67.
3 W. Schumann, W.W. Du Mont and B. Wöbke, J. Organomet. Chem., 128 (1977) 187.
4 A.G. Davies, L. Smith and P. Smith, J. Organomet. Chem., 29 (1971) 245.
5 T.J. Karol, J.P. Hutchinson, J.R. Hyde, H.G. Kuivila and J.A. Zubieta, Organometallics, 2 (1983) 106.
6 K. Jurkschat and M. Gielen, Bull. Soc. Chim. Belg., 91 (1982) 803.
7 M. Gielen, K. Jurkschat, M. Van Meerssche and J. Piret-Meunier, Bull. Soc. Chim. Belg., 93 (1984) 379.
8 M. Gielen and K. Jurkschat, J. Organomet. Chem., 273 (1984) 303.
9 R.G. Swisher and R.R. Holmes, Organometallics, 3 (1984) 365.
10 M. Dräger, J. Organomet. Chem., 251 (1983) 209.
11 A. Tzschach, H. Weichmann and K. Jurkschat, J. Organomet. Chem., Libr., 12 (1981) 293.
12 A. Tzschach, K. Jurkschat, M. Scheer, J. Meunier-Piret, M. Van Meerssche, J. Organomet. Chem., in press.
13 M. Dräger, Z. Naturforsch, B, 36 (1981) 437.
14 M. Dräger, Chem. Ber., 114 (1981) 2051.
15 K. Jurkschat, unpublished results.
16 E.L. Muetterties, J. Am. Chem. Soc., 91 (1969) 1636, 4115.
17 M. Gielen, Meded. Vl. Chem. Veren., 31 (1969) 185.
18 J. Brocas, M. Gielen and R. Willem, The Permutational Approach to Dynamic Stereochemistry, McGraw-Hill Book Company, 1983, Sections 4-2-1 and Chapter 14.
19 Ref. 18, p. 59.
20 J. Brocas and R. Willem, Bull. Soc. Chim. Belg., 82 (1973) 469.
21 J. Brocas and R. Willem, Bull. Soc. Chim. Belg., 82 (1973) 479.
22 C. Mügge, K. Jurkschat, A. Tzschach and A. Zschunke, J. Organomet. Chem., 164 (1979) 135.
23 L. Korecz, A.A. Saghier, K. Burger, A. Tzschach and K. Jurkschat, Inorg. Chim. Acta, 58 (1982) 243 and refs. cited therein.
24 A. Zschunke, A. Tzschach and K. Jurkschat, J. Organomet. Chem., 112 (1976) 273.
25 K. Jurkschat, C. Mügge, A. Tzschach, A. Zschunke, M.-F. Lann, V.A. Pestunovich and M.G. Voronkov, J. Organomet. Chem., 139 (1977) 279.
26 A. Zschunke, C. Mügge, M. Scheer, K. Jurkschat and A. Tzschach, J. Crystall. Spectrosc. Res., 13 (1983) 201 and refs. cited therein.
27 S. Trippett, Phosphorus and Sulfur, 1 (1976) 89.
28 K. Mislow, Acc. Chem. Res., 9 (1976) 26.
29 K. Mislow, D. Gust, P. Finocchiaro and R.J. Boettcher, Top. Curr. Chem., 47 (1974) 1.
30 Ref. 18, Section 9-9.
31 R. Willem, M. Gielen, H. Pepermans, J. Brocas, D. Fastenakel and P. Finocchiaro, J. Am. Chem. Soc., in press.
32 P. Finocchiaro, V. Librando, P. Maravigna and A. Recca, J. Organomet. Chem., 125 (1977) 185.
33 M. Gielen, in G. Geoffroy (Ed.), Topics in Inorganic and Organometallic Stereochemistry, John Wiley, 1981, p. 217.
34 Ref. 3, Sections 13-2-1-1, 13-2-2, 13-2-4-1.
35 M. Gielen and N. Van Lautem, Bull. Soc. Chim. Belg., 79 (1970) 679.
36 R.S. Berry, J. Chem. Phys., 32 (1960) 933.
37 M. Gielen, K. Jurkschat, B. Mahieu and D. Apers, J. Organomet. Chem., in press.
38 P.T. Beurkens, W.P. Bosman, H.M. Doesburg, R.O. Gould, T.E.M. van den Hark and P.A.J. Prick 1980. Tech. Rep. 1980/1. Crystallography Laboratory, Toernooiveld, Nijmegen, The Netherlands.
39 G.M. Sheldrick 1976 SHELX 76. Program for Crystal Structure Determination. University of Cambridge, England.
40 M. Gielen, K. Jurkschat and G. Atassi, Bull. Soc. Chim. Belg., 93 (1984) 153.
41 R.I. Geran, N.H. Greenberg, M.M. MacDonald, A.M. Schumacher and B.J. Abbott, Protocols for screening chemical agents and natural products against animal tumors and other biological systems, Cancer Chemoth. Rep., 3 (1972) 1.